Available online at www.sciencedirect.com
SCIENCE DIRECT
International Journal of Heat and Mass Transfer 49 (2006) 1403–1411
International Journal of HEAT and MASS TRANSFER
www.elsevier.com/locate/ijhmt

Flows in a fluid layer induced by the combined action of a shear stress and the Soret effect

A. Mahidjiba [a,*], R. Bennacer [b], P. Vasseur [c]

[a] Ouranos, 550 Sherbrooke West Street, 19th Floor, Montréal, QC H3A 1B9, Canada
[b] LEEVAM, Rue d'Eragny, Neuville sur Oise, 95031 Cergy-Pontoise Cedex, France
[c] Department of Mechanical Engineering, École Polytechnique, University of Montreal, C.P. 6079, Succ. 'Down Town', Montréal, QC H3C 3A7, Canada

Received 15 April 2005; received in revised form 27 September 2005
Available online 15 December 2005

Abstract

Convection in a horizontal fluid layer of a binary mixture is studied analytically and numerically. In the formulation of the problem, use is made of the Boussinesq approximation. Neumman boundary conditions are specified for the temperature on all walls of the cavity. In addition of the Soret contribution, a shear stress, τ, is applied on the upper free surface of the layer. The flows are found to be dependent of the Darcy–Rayleigh number, R_T, the Lewis number, Le, the solutal to thermal buoyancy ratio, φ, the shear stress, τ and the thermal boundary conditions. Numerical results for finite amplitude convection, obtained by solving numerically the full governing equations, are found to be in good agreement with the analytical solution based on the parallel flow approach. For given sets of the control parameters, the occurrence of multiple steady state solutions is demonstrated. The existence of subcritical bifurcations for both stabilizing and destabilizing mass flux is also demonstrated.
© 2005 Elsevier Ltd. All rights reserved.

Keywords: Double-diffusive convection; Soret contribution; Shear stress; Neumman boundary; Fluid layer

1. Introduction

The existence of convection in double-diffusive systems, in which two substances, e.g. heat and salt, diffuse at different rates, was first recognized in the late 1950. Since then, this phenomena has been studied extensively due to the fact that its importance has been recognized in fields as diverse as geophysics, astrophysics, ocean physics and industrial processes [1–4].

The first study concerning double diffusion in a binary fluid seems to be due to Nield [5]. Relying on the linear stability theory, the onset of motion in an initially motionless, stable concentration stratified horizontal fluid layer heated from the bottom was predicted by this author. Later Veronis [6] and Baines and Gill [7] also relied on linear stability theory to determine the thresholds of convection for various boundary conditions. Non-linear stability theories have also been used by Veronis [8], Huppert and Moore [9] and Knobloch and Proctor [10] to predict the thresholds for finite amplitude convection. Numerical results concerning thermohaline convection in a horizontal layer have been obtained by a few authors (see for instance [11–13]).

All the above studies are concerned with the effect of the regular diffusion of each component (heat and salt) on convection. However, in a wide variety of natural and industrial situations, besides the usual diffusion, cross-diffusion between the two agents may also be important. This phenomena, known as the Soret effect, has been relatively less studied despite its importance in the stability and convection in a fluid layer of a binary mixture. A recent review on the literature in this area is given by Joly et al. [14].

* Corresponding author.
E-mail address: mahidjiba.ahmed@ouranos.ca (A. Mahidjiba).
URLs: http://www.ouranos.ca (A. Mahidjiba), http://www.meca.polymtl.ca/convection (P. Vasseur).

0017-9310/$ - see front matter © 2005 Elsevier Ltd. All rights reserved.
doi:10.1016/j.ijheatmasstransfer.2005.09.034

Nomenclature

A	aspect ratio of the enclosure, L'/H'
a	lateral heating intensity
b	bottom heating intensity
C_S	dimensionless concentration gradient in x-direction, Eq. (16)
C_T	dimensionless temperature gradient in x-direction, Eq. (15)
D	mass diffusivity
D_S	Soret diffusivity
g	gravitational acceleration
H'	height of the enclosure
j'	constant mass flux per unit area
k	thermal conductivity of the fluid
L'	width of the cavity
Le	Lewis number, α/D
Nu	Nusselt number, Eq. (13)
Pr	Prandtl number, ν/α
q'	constant heat flux per unit area
R_T	thermal Rayleigh number, $g\beta_{T'}\Delta T' H'^3/(k\alpha\nu)$
S	dimensionless concentration, $(N-N_0)/\Delta N$
Sh	Sherwood number, Eq. (13)
t	dimensionless time, $t'/(\sigma H'^2/\alpha)$
T	dimensionless temperature, $(T'-T'_0)/\Delta T'$
$\Delta T'$	characteristic temperature, $q'H'/k$
ΔN	characteristic dimensionless concentration, $-N_0(1-N_0)\Delta T' D_S/D$
(x,y)	dimensionless coordinate system, x'/H', y'/H'
(u,v)	dimensionless velocity components, $u'/(\alpha/H')$, $v'/(\alpha/H')$

Greek symbols

α	thermal diffusivity, $k/\rho C$
β_N	solutal expansion coefficient
$\beta_{T'}$	thermal expansion coefficient
φ	buoyancy ratio, $\beta_N\Delta N/\beta_{T'}\Delta T'$
ν	kinematics viscosity of fluid
ρ	density of fluid
ρC	heat capacity of fluid
τ'	shear stress
Ψ	dimensionless stream function, Ψ'/α

Superscript

$'$	dimensionless variable

Subscripts

C	refers to the center of the cavity
S	solutal
T	temperature
0	reference state

Recently, the Soret effect on convection in a horizontal layer of fluid has been investigated both analytically and numerically by Mahidjiba et al. [15]. The influence of various hydrodynamic boundary conditions imposed on the horizontal walls of the layer was studied. The main purpose of this work is to extend the above investigation for the case where a constant shear stress is applied on the upper surface of the layer. Such a condition, which can be encountered in practical situations, has been relatively not studied, particularly in the context of convection of binary mixtures.

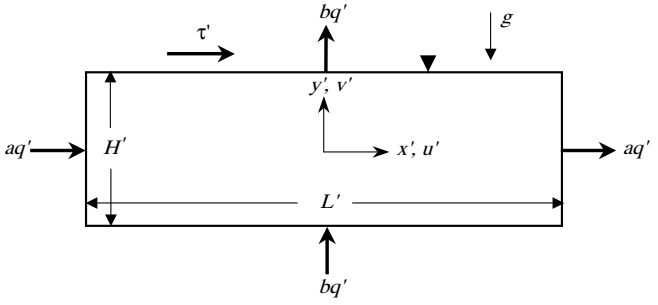

Fig. 1. Geometry of the physical problem.

2. Mathematical formulation

In this investigation, convection within a two-dimensional horizontal cavity filled by an incompressible Newtonian binary fluid (Fig. 1) is studied. The top and bottom horizontal boundaries are subject to uniform fluxes of heat bq', per unit area, while the vertical walls are subjected to heat fluxes aq', where a and b are constants. A shear stress, τ', is applied on the top horizontal free surface while the bottom one is assumed to be rigid. In this study, the Soret effect is taken into consideration. The binary mixture is modeled as a Boussinesq incompressible fluid, having an initial uniform concentration N_0 with physical properties assumed constant, except for the density, which varies with temperature and concentration according to

$$\rho = \rho_0\left[1-\beta_{T'}\left(T'-T'_0\right)-\beta_S(N-N_0)\right] \tag{1}$$

where ρ_0 is the reference fluid density at temperature $T'=T'_0$ and concentration $N=N_0$, and $\beta_{T'}$ and β_N are the thermal and concentration expansion coefficients, respectively.

The mass transfer, taking in account the Soret effect, is given by

$$J' = -\rho D\nabla N - \rho D_S N_0(1-N_0)\nabla T' \tag{2}$$

where D represents the mass diffusivity and D_S the Soret effect.

In the present study The Dufour effect, i.e. heat transfer driven by a concentration gradient, is neglected as usual. This parameter can be important in binary gas mixtures but is negligible in binary liquid mixtures [16].

The dimensionless governing equations are the momentum, energy and concentration equations given as

$$\frac{\partial \nabla^2 \Psi}{\partial t} + J\left(\Psi, \nabla^2 \Psi\right) = Pr\nabla^4 \Psi - PrR_T \frac{\partial}{\partial x}(T + \varphi S) \tag{3}$$

$$\frac{\partial T}{\partial t} + J(\Psi, T) = \nabla^2 T \tag{4}$$

$$\frac{\partial S}{\partial t} + J(\Psi, S) = \frac{1}{Le}\left(\nabla^2 S - \nabla^2 T\right) \tag{5}$$

where J is expressed as $J(f,g) = f_y g_x - f_x g_y$. The functions f and g stand for any physical variable (Ψ, T or S).

The unknown variables are the components (u,v) of the mass averaged velocity $\vec{V}$, temperature T and concentration S. The stream function Ψ, related to the velocity components as $u = \partial\Psi/\partial y$ and $v = -\partial\Psi/\partial x$, is introduced so that the continuity equation is automatically satisfied. The above equations were obtained by using the following dimensionless quantities:

$$\begin{aligned} &(x,y) = (x',y')/H' \quad (u,v) = (u',v')/(\alpha/H') \quad t = t'/\left(H'^2/\alpha\right) \\ &\Psi = \Psi'/\alpha \quad T = \left(T' - T'_0\right)/\Delta T' \quad \Delta T' = q'H'/k \\ &S = (N - N_0)/\Delta N \quad \Delta N = -D_S N_0 (1 - N_0)\Delta T'/D \end{aligned} \tag{6}$$

where t is the dimensionless time, α the thermal diffusivity and k the thermal conductivity.

The dimensionless thermal and concentration boundary conditions are

$$x = \pm A/2 \quad \frac{\partial T}{\partial x} = \frac{\partial S}{\partial x} = -a \tag{7}$$

$$y = \pm 1/2 \quad \frac{\partial T}{\partial y} = \frac{\partial S}{\partial y} = -b \tag{8}$$

The dimensionless hydrodynamic boundary conditions for the vertical walls are

$$x = \pm A/2 \quad \Psi = 0 \tag{9}$$

$$y = -1/2 \quad \Psi = \frac{\partial \Psi}{\partial y} = 0 \tag{10}$$

$$y = 1/2 \quad \Psi = 0 \quad \tau = \frac{\partial^2 \Psi}{\partial y^2} \tag{11}$$

where $\tau = \tau' H'^2/\alpha\mu$ is the dimensionless shear stress and $A = L'/H'$ is the cavity aspect ratio.

It is noted that that the present system is governed by the thermal Darcy–Rayleigh number, R_T, the solutal to thermal buoyancy ratio, φ, the Prandtl number, Pr, the Lewis number, Le, the heating mode, a and b, the cavity aspect ratio, A, and the dimensionless shear stress, τ. These parameters are defined as

$$\begin{aligned} &R_T = \frac{g\beta_{T'}\Delta T' H'^3}{\alpha v} \quad \varphi = \frac{\beta_N \Delta N}{\beta_{T'}\Delta T'} \quad \tau = \frac{\tau' H'^2}{\alpha\mu} \\ &Pr = \frac{v}{\alpha} \quad Le = \frac{\alpha}{D} \quad A = \frac{L'}{H'} \end{aligned} \tag{12}$$

It is noted that the thermal coefficient, $\beta_{T'}$, is usually a positive quantity. On the other hand, the solutal coefficient β_N can be positive ($\varphi > 0$) or negative ($\varphi < 0$). For $\varphi > 0$, the thermal and solutal boundary forces are both destabilizing. Thus, the two buoyancy components make aiding contributions. For $\varphi < 0$ they make opposing contributions. However, the Nusselt and Sherwood numbers, characterizing the heat and mass transfers, respectively, are defined by

$$Nu = 1/\Delta T \quad \text{and} \quad Sh = 1/\Delta S \tag{13}$$

where $\Delta T = T(0,-1/2) - T(0,1/2)$ is the temperature difference, evaluated at $x = 0$, between the two horizontal boundaries. $\Delta S = S(0,-1/2) - S(0,1/2)$ is the concentration difference. In the above equations Nu represents, as usual, the heat transfer across (ΔT) the walls of the cavity resulting from the combined action of convection and conduction. However, because the walls of the cavity are impermeable, Sh does not have its usual significance. Here, it is rather related to the concentration distribution within the cavity induced by the Soret effect and by convection.

3. Numerical solution

To solve numerically the governing equations, a control volume approach is used. The SIMPLER algorithm is employed to solve the equations in primitive variables. Central differences are used to approximate the advection-diffusion terms (see Mahidjiba et al. [15] for more details). The criteria of convergence are to conserve mass, momentum energy and species globally and locally, and to insure convergence of pre-selected dependent variables to constant values within machine error at each time step. The difference obtained with these grids was less than 1% in Nu, Sh and Ψ_C. Thus, most of the calculations presented in this paper were performed using a 61×181 grid. The solution is assumed to be converged when the error is less than 10^{-7}. All results presented here were obtained for $A = 12$ and $Pr = 1$.

4. Analytical solution

For the case of an infinite layer, the problem can be solved analytically by using the parallel flow approximation in the center of the cavity. The following transformations are introduced

$$\Psi(x,y) \approx \Psi(y) \tag{14}$$

$$T(x,y) = C_T x + \theta_T(y) \tag{15}$$

$$S(x,y) = C_S x + \theta_S(y) \tag{16}$$

where C_T and C_S are unknown constants associated, respectively, with the temperature and the concentration gradients in x-direction. θ_T and θ_S are, respectively, the temperature and concentration profiles in the vertical direction (see, for instance [17]).

Substituting Eqs. (14)–(16) into Eqs. (3)–(5), yields the following set of equations:

$$\frac{d^4\Psi}{dy^4} = \Psi_0 \quad \text{where } \Psi_0 = R_T(C_T + \varphi C_S) \tag{17}$$

$$\frac{d^2\theta_T}{dy^2} = C_T\frac{d\Psi}{dy} \tag{18}$$

$$\frac{d^2\theta_S}{dy^2} - \frac{d^2\theta_T}{dy^2} = C_S Le\frac{d\Psi}{dy} \tag{19}$$

According to Kimura and Bejan [18], the boundary conditions in x-direction can be approximated by an equivalent energy flux condition in x-direction for the temperature and concentration, given by

$$C_T + a = \int_{-1/2}^{1/2} u\theta_T\,dy \tag{20}$$

$$C_S - C_T = Le\int_{-1/2}^{1/2} u\theta_S\,dy \tag{21}$$

The analytical resolution of Eqs. (17)–(19), subject to boundary conditions (7)–(11), gives

$$\Psi(x,y) = \frac{1}{24}\left[\Psi_0 y^4 - \frac{\Psi_1}{2}y^3 - \frac{3\Psi_3}{4}y^2 + \frac{\Psi_1}{8}y + \frac{\Psi_2}{8}\right] \tag{22}$$

$$T(x,y) = C_T x + \frac{C_T}{24}\left(\frac{\Psi_0}{5}y^5 - \frac{\Psi_1}{8}y^4 - \frac{\Psi_3}{4}y^3 + \frac{\Psi_1}{16}y^2 + \frac{\Psi_2}{8}y\right) - by \tag{23}$$

$$S(x,y) = C_S x + \frac{(LeC_S + C_T)}{24}\left(\frac{\Psi_0}{5}y^5 - \frac{\Psi_1}{8}y^4 - \frac{\Psi_3}{4}y^3 + \frac{\Psi_1}{16}y^2 + \frac{\Psi_2}{8}y\right) - by \tag{24}$$

where $\Psi_1 = \Psi_0 - 12\tau$, $\Psi_2 = \Psi_0 - 6\tau$ and $\Psi_3 = \Psi_0 - 4\tau$.

The unknown constants C_T and C_S can be found by substituting Eqs. (22)–(24) into Eqs. (20) and (21) and performing the resulting integrations. They are given by

$$C_T = \frac{\beta_1\gamma - (\beta_2\tau + a)}{1 + \beta_2\tau Z/5 + \beta_3\gamma^2} \tag{25}$$

$$C_S = \frac{C_T\{1 - Le\lfloor\beta_2\tau Z/5 + \beta_3\gamma^2\rfloor\} + Le(\beta_1\gamma - \beta_2\tau)}{1 + Le^2[\beta_2\tau Z/5 + \beta_3\gamma^2]} \tag{26}$$

where $\gamma = \Psi_0/24$, $\beta_1 = 3b/40$, $\beta_2 = 1/48$, $\beta_3 = 19/(4\times 630)$ and $Z = (\tau/7 - \gamma)$.

Upon combining the above equations with the definition of Ψ_0 it is readily found:

$$A_0 + A_1\gamma + A_2\gamma^2 + A_3\gamma^3 + A_4\gamma^4 + A_5\gamma^5 = 0 \tag{27}$$

where

$$A_0 = 1225aR_T(N+1) + 35\beta_2 R_T\left[35[N(1+Le)+1]\tau. + aLe(Le-N)\tau^2 + \beta_2 Le^2\tau^3\right]$$

$$A_1 = \begin{pmatrix} 1225[24 - \beta_1 R_T(N(Le+1)+1)] + 245a\beta_2 R_T Le(N-Le)\tau \\ +35\beta_2\left[24 + Le^2(24 - R_T(7\beta_2 + \beta_1))\right]\tau^2 + 24\beta_2^2 Le^2\tau^4 \end{pmatrix}$$

$$A_2 = \begin{pmatrix} 1225aR_T\beta_3 Le(Le-N) + 245\beta_2\left[(5R_T\beta_3 + R_T\beta_1 - 24)Le^2 - 24\right]\tau \\ -336\beta_2^2 Le^2\tau^3 \end{pmatrix}$$

$$A_3 = \begin{pmatrix} 24\beta_2(49\beta_2 + 70\beta_3)Le^2\tau^2 \\ 1225\beta_3\left[24(1+Le^2) - R_T\beta_1 Le^2\right] \end{pmatrix}$$

$$A_4 = -11760\beta_2\beta_3\tau Le^2 \quad A_5 = 24(35\beta_3 Le)^2$$

The non-linear equation (27) can be solved numerically by using for instance the Muller's method for given values of R_T, Le, φ, a and τ.

From Eqs. (23), (24) and (13), the Nusselt and Sherwood numbers are

$$Nu = \frac{1}{1 + C_T(\beta_2\tau - \beta_1\gamma)} \tag{28}$$

$$Sh = \frac{1}{1 + (LeC_S + C_T)(\beta_2\tau - \beta_1\gamma)} \tag{29}$$

5. Results and discussion

As discussed above, the present problem depends upon the parameters: R_T, φ, τ, Pr, Le, A, a and b. The analytical model is valid asymptotically for a shallow cavity ($A \gg 1$). Also, the cavity is assumed to be always heated from the bottom such that $b = 1$.

5.1. Case of a cavity not heated from the vertical sides ($a = 0$)

The influence of the buoyancy ratio, φ on the stream function at the center of cavity, Ψ_C, is illustrated in Fig. 2 for $Le = 10$. It is observed that the analytical model (solid and dashed lines) is in general in very good agreement with the numerical results represented by symbols. Fig. 2a is plotted for $\tau = 0$ (no shear stresses applied on the top of the layer) and for different values of the Rayleigh number R_T ($R_T = 10^3$, 2×10^3 and 4×10^3). For this situation, the fluid layer is heated from the bottom and convection is possible only for R_T above a critical value $R_T(1 + \varphi Le) \geqslant 320$. Thus, the critical buoyancy ratio for the onset of supercritical convection φ_{Cr} is given by

$$\varphi_{Cr} \geqslant (320/R_T - 1)/Le \tag{30}$$

Fig. 2a indicates for a given φ above the critical value φ_{Cr} (which depends upon, R_T), the flow rotates indifferently clockwise or counterclockwise. In addition, it is noticed that with the thermal boundary conditions considered here (constant fluxes) the resulting flow pattern is unicellular. This is not the case of a cavity heated isothermally from the bottom for which it is well known that the resulting flow pattern is multicellular. In Fig. 2a it is observed that when the solutal and the thermal buoyancy forces are both destabilizing ($\varphi > 0$) convection is always possible

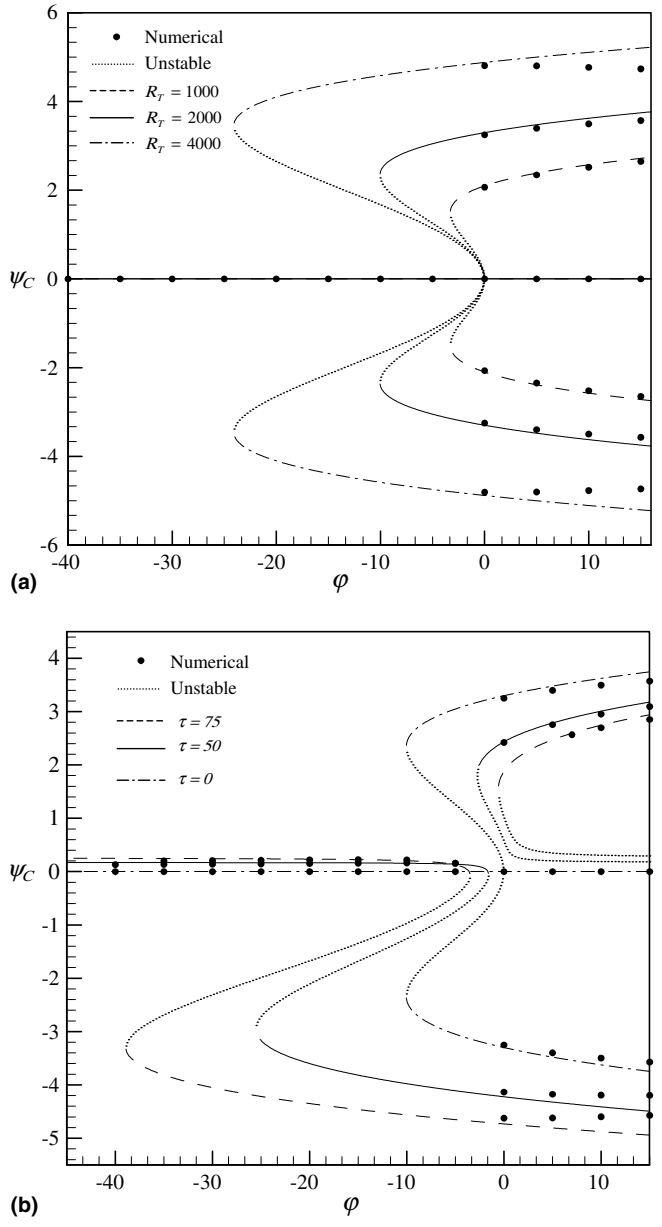

Fig. 2. Effect of buoyancy ratio, ϕ on the stream function at the center of cavity for $a = 0$, $Le = 10$ and (a) $\tau = 0$ and different values of R_T ($R_T = 10^3$, 2×10^3 and 4×10^3) and (b) $R_T = 2 \times 10^3$ and different values of τ ($\tau = 0$, 50 and 75).

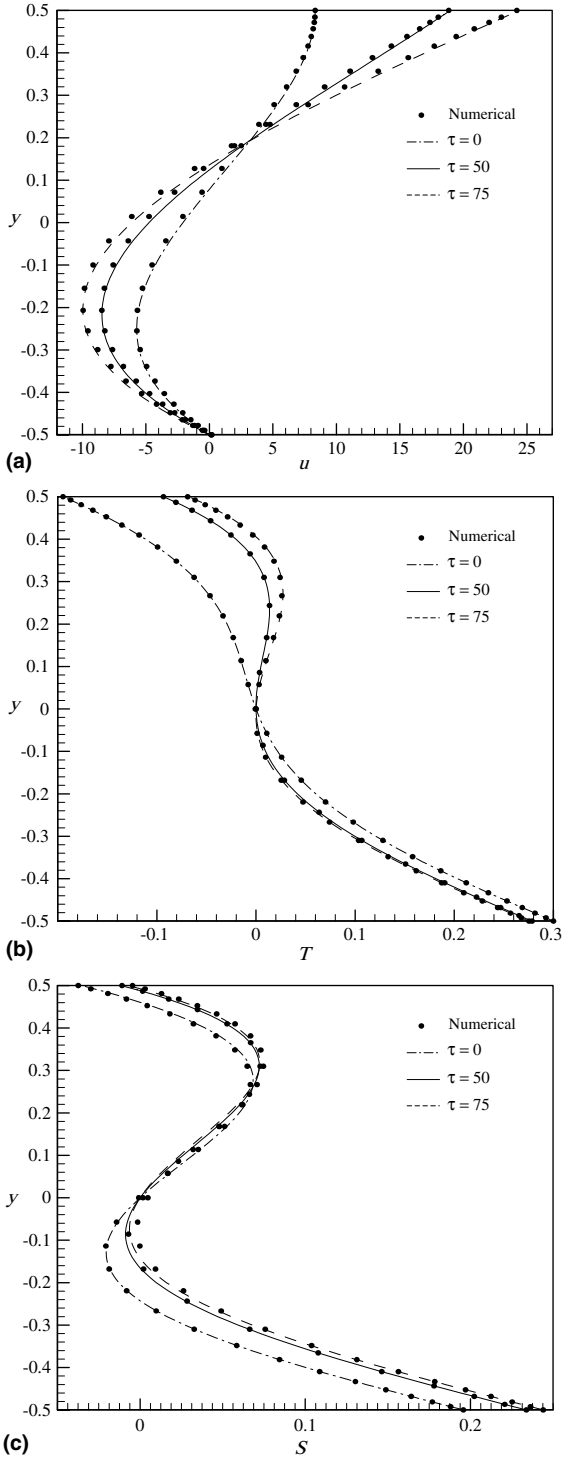

Fig. 3. Distribution of (a) horizontal velocity component, u, (b) temperature, T, and (c) concentration, S, profiles at the vertical mid-plan ($x = 0$) of the cavity for $a = 0$, $R_T = 10^3$, $Le = 10$, $\varphi = -0.2$ and for different values of τ ($\tau = 0$, 50 and 75).

independently of the value of φ. However, for $\varphi < 0$, i.e. when the thermal buoyancy forces are destabilizing while the solutal ones are stabilizing, convection occurs only when φ is greater than a value that depends upon R_T. Thus, convection is possible above $\varphi > -0.068$ when $R_T = 10^3$ and above $\varphi > -0.092$ when $R_T = 4 \times 10^3$. The occurrence of subcritical bifurcations, for which convection occurs at finite amplitude, is noted for this situation.

Fig. 2b illustrates the effect of the shear stress, τ, for $R_T = 2 \times 10^3$. For $\tau = 0$, the situation is the same as that discussed above. The flow can rotate indifferently clockwise or counterclockwise, the two results being perfectly symmetrical. For $\tau \neq 0$, the solutions are, as expected, not symmetrical. For a given value of τ, it is observed that in general three solutions are possible for a given value of φ. Thus for $\varphi > 0$, the analytical model predicts the existence of a clockwise unicellular flow ($\Psi_C < 0$) induced by the shear stress applied on the upper free boundary.

Furthermore, it is seen that an anticlockwise unicellular flow ($\Psi_C > 0$) is also predicted by the analytical model. This follows from the fact that for $\tau = 0$ both clockwise and anticlockwise circulations are possible. These two types of circulation can also be maintained provided that the value of τ is made not too large. Similarly for $\varphi < 0$ solutions are possible for both $\Psi_C > 0$ or $\Psi_C < 0$. The circulation induced in the direction imposed by the shear force will be called natural and that in the opposed direction anti natural in the following discussion.

The distribution of the velocity component, u, temperature, T, and concentration, S, profiles in the vertical midplane ($x = 0$) of the cavity is illustrated in Fig. 3. This graph has been plotted for $R_T = 10^3$, $Le = 10$, $N = -0.2$ and for different values of the shear stress, τ ($\tau = 0$, 50

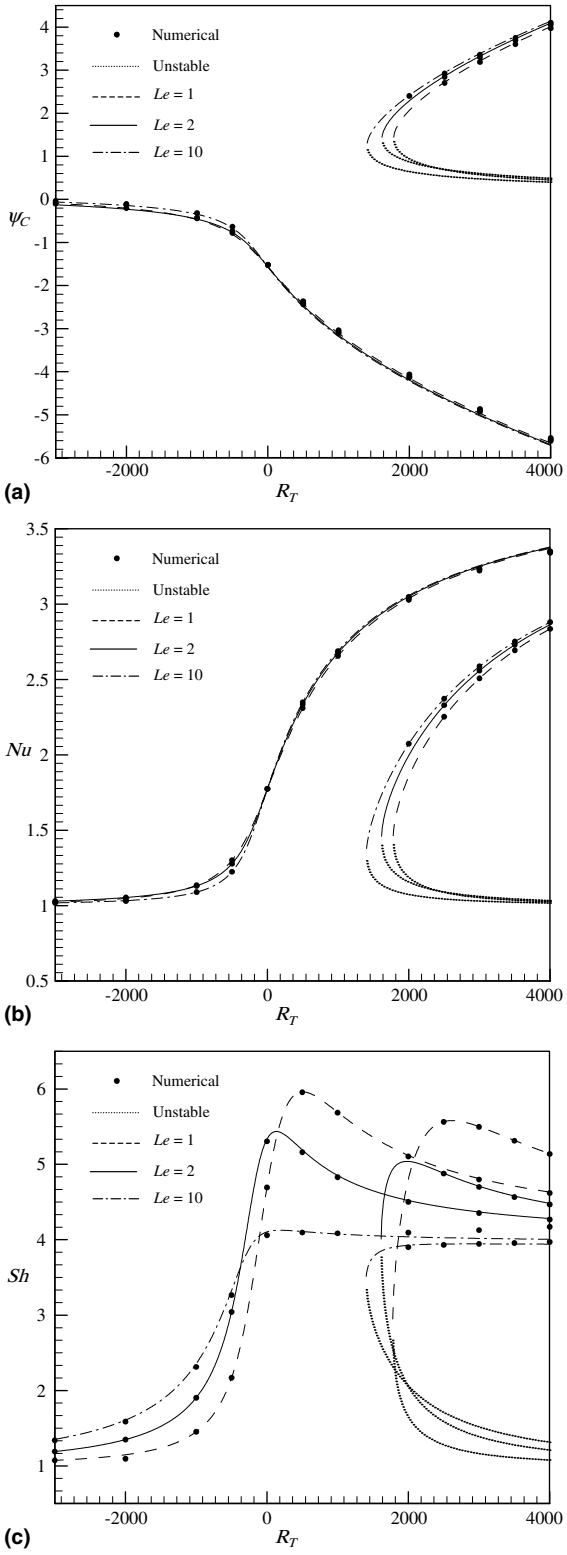

Fig. 4. Effect of the Rayleigh number, R_T on the (a) stream function at the center of cavity, (b) Nusselt number and (c) Sherwood number for $a = 0$, $Le = 10$, $\tau = 50$, $\varphi = -0.2$ and different values of Lewis number, Le ($Le = 1$, 2 and 10).

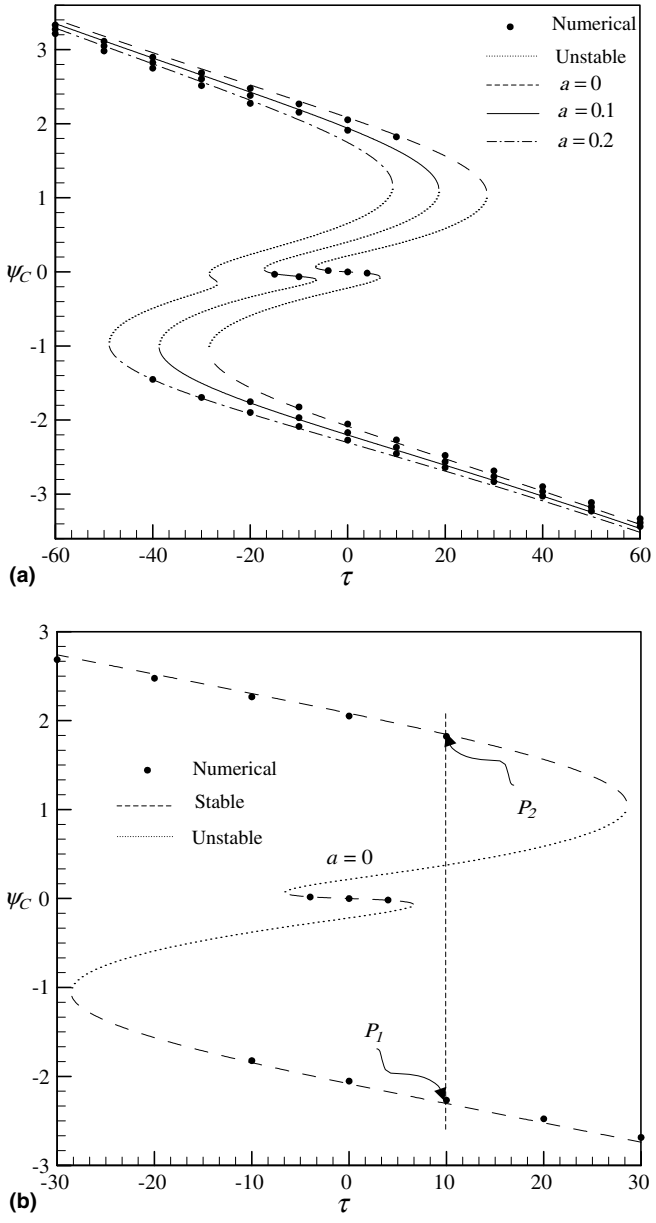

Fig. 5. Effect of the shear stress, τ on the: (a) stream function at the center of cavity and (b) zoom of the case $a = 0$ for $Le = 10$, $R_T = 10^3$, $\varphi = -0.2$ and for different values of a ($a = 0$, 0.1 and 0.2).

and 75). The results show that the numerical approach (dotted symbols) is in excellent agreement with the analytical model (solid and dashed lines), based on the parallel flow approximation. The effect of the shear stress is clearly observed in this figure. The intensity of the flow (velocity) increases considerably near the upper surface when the shear stress, τ is made larger. The influence of τ is found to be larger on the temperature, T, and than on the concentration, S.

Fig. 4 illustrates the influence of the Rayleigh number, R_T on Ψ_C, Nu and the Sherwood number, Sh for $\tau = 50$ and $\varphi = -0.2$ and different values of the Lewis number, Le ($Le = 1$, 2 and 10). Here again it is noted that the numerical and analytical results are in a good agreement. For $R_T > 0$, it is seen that the natural branch ($\Psi_C < 0$) exists for any value of the Rayleigh number, the intensity of Ψ_C increasing monotonously with R_T. On the other hand, the antinatural branch ($\Psi_C > 0$) is possible only when R_T is above a critical value that depends upon the Lewis number, Le. Thus, the antinatural branch is obtained at $R_T \approx 1405$ for $Le \geqslant 10$, $R_T \approx 1615$, for $Le = 2$ and $R_T \approx 11780$ for $Le = 1$. The antinatural solution contains a stable branch (solid line) and an unstable one (dotted line). The numerical model predicts only existence of the stable branch. Also it is noted that, independently of the value of the Lewis number, Le, all the natural branches merge approximately on a same curve. However, the effect of the Lewis number, Le, on the stream function, Ψ_C, is clearly observed to be more significant for the case of the antinatural solutions. For sufficiently large value of the Rayleigh number, R_T, ($R_T > 3 \times 10^3$), this effect disappears and the three curves have again a tendency to merge on a single curve. The effect of the Lewis number on the heat transfer (Nu) is also observed to be negligible excepted near the turning points of the antinatural branches. On the other hand, in the case of the Sherwood number, the Lewis number is seen to be more significant.

5.2. Case of a cavity heated from the vertical sides ($a \neq 0$)

The effect of the shear stress, τ, on the stream function at the center of cavity, Ψ_C is discussed in Fig. 5a for $R_T = 10^3$, $Le = 10$, $\varphi = -0.2$ and $a = 0$, 0.1 and 0.2. When $a = 0$ (dashed line), i.e. when the layer is heated only from below, the results show the existence of two solutions, clockwise and anticlockwise circulation. For this situation, which has been discussed above, the results show that independently of the value and the direction of the shear stress, τ, the convective flow is mirror case (antisymmetric) (see Fig. 5b). The occurrence of unstable branches of solution between $\tau \approx -28.5$ and 6.56 is indicated by a dashed line. To examine the effect of the lateral heating, a, on the solution, different values of a ($a = 0.1$ and 0.2) are imposed on the vertical walls of the cavity. It is seen that the natural solution (anticlockwise circulation, $\Psi_C < 0$) and antinatural one (clockwise circulation, $\Psi_C > 0$) are also possible for a range value of the shear stress, τ. However, these solutions are not symmetric as for the classical Bénard problem ($a = 0$) because of the effect of the lateral heating. For high values of $|\tau|$, all results merge approximately on the same curve for any value of a.

Fig. 6 illustrates the set of contour lines for Ψ, T and S obtained numerically for $R_T = 10^3$, $Le = 10$, $\varphi = -0.2$, $a = 0$ and $\tau = 10$. Fig. 6a corresponds to natural clockwise circulation ($\Psi_C < 0$) and Fig. 6b to antinatural anticlockwise circulation ($\Psi_C > 0$). These two solutions are identified by P_1 and P_2, respectively, in Fig. 5b. These results show that the flow is parallel in the core of the cavity and the temperature and concentration are linearly stratified in the horizontal direction.

Fig. 7 illustrates the number of solutions obtained for a given set value of parameters, a ($a = 0.05$), Le ($Le = 10$), R_T ($R_T = 2 \times 10^3$), φ and τ. The existence of three different regions corresponding to one, tree and five solutions,

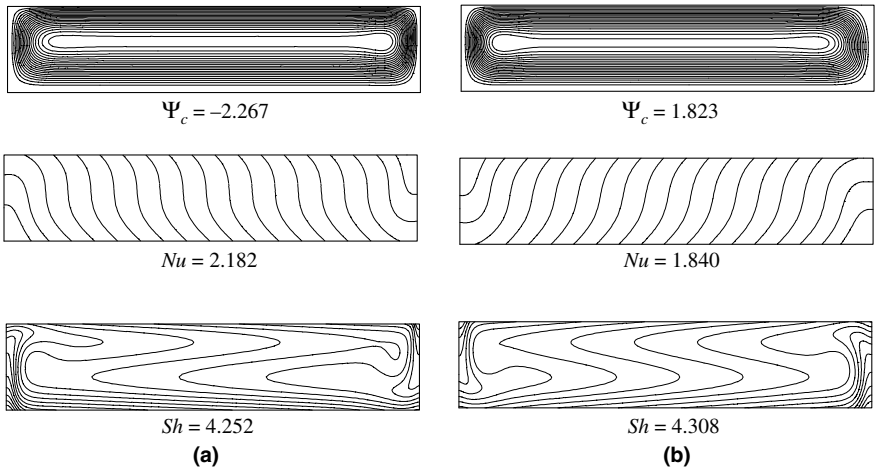

Fig. 6. Contour lines of stream function, temperature and concentration for $a = 0$, $R_T = 10^3$, $Le = 10$, $\varphi = -0.2$ and $\tau = 10$: (a) antinatural flow (P_1) and (b) antinatural flow (P_2).

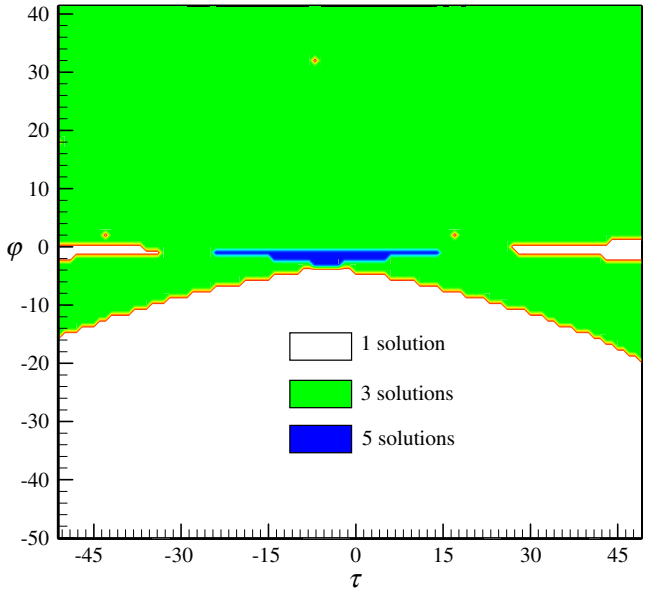

Fig. 7. Illustration of the number of solutions obtained for the case $a = 0.05$, $Le = 10$, $R_T = 2 \times 10^3$ and for different values of φ and τ.

respectively, is observed. The zone of one solution is obtained for $\varphi < 0$ or for $|\varphi| \ll 1$. The case of $\varphi < 0$ corresponds to the diffusive solution, which prevails for any value of τ. However, we have also a one solution domain in the case of $|\varphi| \ll 1$ obtained only for large values of τ. This situation corresponds to the solutal Rayleigh–Bénard solution where there is only one flow circulation imposed by the shear stress applied on the free surface. The zone of five solutions is obtained for $|\varphi| \ll 1$ and for moderate values of τ. This zone corresponds to the existence of the pure Rayleigh–Bénard solution (rotating indifferently in the two directions), the diffusive solution (no flow) and two unstable solutions corresponding to the subcritical bifurcations. The last zone corresponds to the region of three solutions. This region, obtained for the solutal destabilizing situation ($\varphi > 0$), corresponds to the existence of a natural branch and an antinatural one with two solutions (one stable and another unstable).

6. Conclusions

The effect of the shear stress, τ, applied on the free upper boundary of a horizontal fluid layer of a binary mixture, with Soret contribution, has been studied both analytically and numerically. Uniform heat fluxes are applied on the boundaries of the system. Using the parallel flow approximation, an analytical model is developed. A finite volume method is used to solve numerically the present problem. This later is found to depend on the aspect ratio of the cavity, A, Lewis number, Le, Prandtl number, Pr, solutal to thermal buoyancy ration, φ, Rayleigh number, R_T, shear stress, τ, and the heating mode (a, b). The main results of the present study are:

1. An approximate analytical model has been derived to predict the flow and the heat and mass transfer for the present problem. The model is found to be in excellent agreement with a numerical solution of the full governing equations.
2. In the absence of the lateral heating ($a = 0$), it is found that the application of a shear stress destroyed considerably the symmetry of the solution obtained for a pure Bénard situation ($\tau = 0$). For a given set of the governing parameters the existence of up to five different solutions (three stable and two stable) has been demonstrated.
3. In the presence of the lateral heating ($a \neq 0$), the results also indicate the existence of multiple solutions for a given set of the governing parameters. However, the symmetry of the flow with respect to $|\tau| = 0$ is naturally destroyed by the lateral heating effects.

Acknowledgements

This work was supported in part by the Natural Sciences and Engineering Research Council, Canada. Part of this work was supported by the 'Ministère de la Recherche de France'.

References

[1] J.S. Turner, Double-diffusive phenomena, Annu. Rev. Fluid Mech. 6 (1974) 37–56.
[2] S. Ostrach, Natural convection with combined driving forces, Physicochem. Hydrodyn. 1 (4) (1980) 233–247.
[3] U. Hansen, D.A. Yuen, Subcritical double-diffusive convection at infinite Prandtl number, Geophys. Astrophys. Fluid Dyn. 47 (1989) 199–224.
[4] R.W. Schmih, Double diffusion in oceanography, Annu. Rev. Fluid Mech. 26 (1994) 236–255.
[5] D.A. Nield, The thermohaline Rayleigh–Jeffreys problem, J. Fluid Mech. 29 (1967) 545–558.
[6] G. Veronis, Effect of a stabilizing in thermohaline convection, J. Fluid Mech. 34 (1968) 315–368.
[7] P.G. Baines, A.E. Gill, On the thermohaline convection with linear gradients, J. Fluid Mech. 37 (1969) 289–306.
[8] G. Veronis, On finite amplitude instability in thermohaline convection, J. Mar. Res. 23 (1965) 1–17.
[9] H.E. Huppert, D.R. Moore, Nonlinear double-diffusive convection, J. Fluid Mech. 78 (1976) 821–854.
[10] E. Knobloch, M. Proctor, Nonlinear periodic convection in double-diffusive systems, J. Fluid Mech. 108 (1981) 291–316.
[11] A.A. Predtechensky, W.D. McCormick, J.B. Swiff, A.G. Rossberg, H.L. Swinney, Traveling wave instability in sustained double-diffusive convection, Phys. Fluid. 6 (1994) 3923–3935.
[12] A. Spina, J. Toomre, E. Knobloch, Confined states in large-aspect-ratio thermohaline convection, Phys. Rev. E 57 (1998) 524–545.
[13] M. Mamou, P. Vasseur, M. Hasnaoui, On numerical stability analysis of double-diffusive convection in confined enclosure, J. Fluid Mech. 433 (2001) 209–250.
[14] F. Joly, P. Vasseur, G. Labrosse, Soret instability in a vertical Brinkman porous enclosure, Numer. Heat Transfer 39 (2001) 339–359.

[15] A. Mahidjiba, R. Bennacer, P. Vasseur, Effect of the boundary conditions on convection in a horizontal fluid layer with Soret contribution, Acta Mech. 160 (2003) 161–177.
[16] St. Hollinger, M. Lucke, Influence of the Dufour effect on convection in binary gas mixtures, Phys. Rev. E 52 (1995) 642–657.
[17] M. Mamou, P. Vasseur, E. Bilgen, Double-diffusive convection instability in a vertical porous enclosure, J. Fluid Mech. 368 (1998) 263–289.
[18] S. Kimura, A. Bejan, The boundary-layer natural convection regime in a rectangular cavity with uniform heat flux from the side, J. Heat Transfer 106 (1984) 98–103.